Progress In Electromagnetics Research C, Vol. 33, 133–144, 2012

A SRR-BASED NEAR FIELD RFID ANTENNA

X.-Z. Lai[1, *], Z.-M. Xie[2], Q.-Q. Xie[2], and J.-W. Chao[2]

[1]School of Computer Science & Engineering, South China University of Technology, Guangzhou 510006, China

[2]School of Electronic & Information, South China University of Technology, Guangzhou 510006, China

Abstract—In this paper, a compact near field reader antenna is proposed for ultra-high frequency (UHF) radio frequency identification (RFID) applications. The antenna structure is composed of two split-ring-resonators (SRRs) and miniaturized to a special small size of $21 * 21 * 1.6\,\mathrm{mm}^3$ for mobile RFID application. The measured bandwidth of antenna prototype is 13 MHz (914.5–927.5 MHz) with reflection coefficient less than -10 dB, which covers the China RFID band II (920–925 MHz). Simulation shows that the proposed antenna achieves a strong and uniform magnetic field distribution in the near field region, and the reading range is up to 42 mm with near field RFID tag. Through modifying the parameters of SRRs, the antenna can operate on different UHF RFID bands (Europe band, China band I&II etc.).

1. INTRODUCTION

Radio-frequency-identification (RFID) has played a major role for automated identifying and tracking objects in various applications, such as warehouse, supply chain, industry, and commerce [1]. Generally, there are two kinds of RFID systems: far-field and near-field system. The far-field RFID systems only operate at UHF (840–960 MHz) bands with electromagnetic waves propagating between the readers and tags. Relatively, the near-field RFID systems are based on inductive coupling to transfer power and transmit data between the readers and tags. In near-field systems, the inductive coupling stores most of the reactive energy in the magnetic field near to the reader antenna region. Compared to the far-field system, the advantage of

Received 19 August 2012, Accepted 28 September 2012, Scheduled 3 October 2012
* Corresponding author: Xiao-Zheng Lai (laixz@scut.edu.cn).

near-field system is that the reader antenna will be only affected by high magnetic permeability objects and operates well in close proximity to metals and liquid [2]. The near-field systems can operate at low frequency (LF, 125–134 kHz), high frequency (HF, 13.56 MHz) and UHF bands. The conventional LF/HF near-field RFID tag has complex multiturn loop structure, and the data transmission rate is lower compared to UHF near-field systems. Therefore, much effort has been devoted to the development of UHF near-field RFID technology, and a group of near-field reader antenna structures has been considered. Almost [3–9] are designed for having in-phase current even though the perimeter of the loop is comparable to the operating wavelength, as the biggest area is $154 * 154\,\mathrm{mm}^2$ [4] and the smallest is $80 * 70\,\mathrm{mm}^2$ [8]. Only a few researches have been done on minimizing the size: one has a dimension of $26 * 26\,\mathrm{mm}^2$ and bandwidth of 5.8 MHz [10]; another has a dimension of $46.5 * 46.5\,\mathrm{mm}^2$ and bandwidth of 10 MHz [11]. The relatively large sizes and relatively narrow band of these antennas make them difficult for mobile RFID application.

In order to address the size constraint problem, we make a tentative suggestion of a novel type of RFID reader antenna for near-field application [12]. In this paper, we present formally the compact SRR-based RFID antenna and give more details of the near-field characteristics by simulation and measurements. The compact antenna prototype is fabricated with a special small size of $21 * 21 * 1.6\,\mathrm{mm}^3$, which is one of the smallest dimension of RFID reader antenna in the world. The measured result of prototype shows good impedance matching over 13 MHz (914.5–927.5 MHz) with reflection coefficient less than -10 dB, which covers the China RFID band II (920–925 MHz). Simulation shows that the antenna features a strong and uniform magnetic field distribution, and agrees well with the reading range of 42 mm. The antenna also operates different UHF RFID bands (Europe band, China band I&II) by modifying the SRR parameters.

The rest of this letter is arranged as follows: The basic theory of SRR is given in Section 2. The antenna structure and design details are presented in Section 3. Section 4 outlines the simulation and measured results, including impedance match bandwidth, current and magnetic field distribution, and reading range. The conclusion is given in Section 5.

2. THEORY OF SRR

Split Ring Resonator (SRR), as shown in Fig. 1, is first proposed by Pendry et al. [13]. It is formed by two different diameter size concentric metal rings with one gap on the opposite position of each one. As a

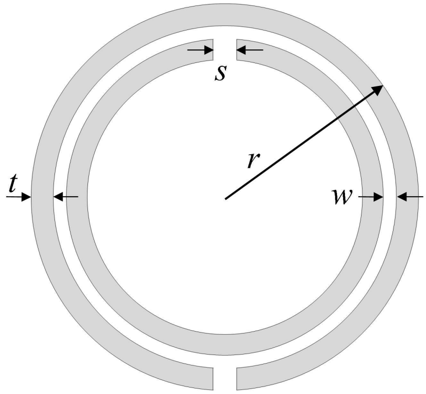

Figure 1. Layout configuration of SRRl.

resonator, the inductive effect of SRR is created by the rings while the capacitive effect is determined by the gap between split rings and the gaps at each ring.

Pendry et al. [13] give the fundamental resonant frequency and wavelength of SRR, as follows:

$$f_{SRR} = \frac{c}{2\pi^2}\sqrt{\frac{3w}{\varepsilon_r(r-2t-w)^3}} \tag{1}$$

$$\lambda_{SRR} = 2\pi^2\sqrt{\frac{(r-2t-w)^3}{3w}} \tag{2}$$

ε_r is the relative permittivity of substrates, r the radius of outer ring, t the width of the metal ring, and w the spacing of the two rings.

In order to minimizing the antenna size, SRR has been used in far-field antenna researches. Kim et al. [10] proposed a small antenna with a capacitive SRR, which has an area of $26 * 26\,\text{mm}^2$ and a narrow impedance bandwidth of 5.8 MHz (901.7–907.5 MHz). Another is a novel design of a compact multi-band planar microstrip antenna presented by Si and Lv [14], which consists of split-ring resonator (SRR) and closed-ring resonator. The structure of the antenna makes low (2.40–2.48 GHz), middle (3.49–3.79 GHz) and high (5.15–5.825 GHz) resonant bands.

It is seen that there is a strong magnetic field near the central axis and close to the resonator, when current in-phase on SRR varies at the resonance frequency. We propose SRR structure in near-field antenna design and obtain significant effect on miniaturization of antenna and good bandwidth.

3. ANTENNA DESIGN AND STRUCTURE

The configuration of proposed antenna is shown in Fig. 2. The SRR structure and ground are respectively fabricated on the opposite sides of the FR-4 substrate with dielectric constant $\varepsilon_r = 4.4$, loss tangent $\delta = 0.02$ and thickness $h = 1.6$ mm.

The SRR structure is formed by two coupled square-rings separated by a gap, each with a split at opposite sides. The fundamental resonant frequency f is expressed as follows,

$$f = \frac{1}{2\pi\sqrt{LC}} \tag{3}$$

SRR consists of capacitive loading and inductive loadings. L is the equivalent inductance loading depends on the length of rings, and C is the equivalent capacitance loading determined by the gap between the rings and the splits at each ring. Both capacitive and inductive loading are simultaneously applied as an LC tank circuit, and resonance characteristic results in antenna size reduction.

On the top view of Fig. 2, $L1$ is the edge side of the fabrication, and $L2$ is the edge of the outer square. Then, g is the gap between the inner and outer, $s1$ is the split width of the inner square, and $s2$ is the outer square. Particularly, the inner square has the same line width $w1$, but the outer square has two different line widths of $w1$ and $w2$. This can broaden the bandwidth of the antenna. Finally, $L4$ is the distance between the feed point and a corner of the outer square.

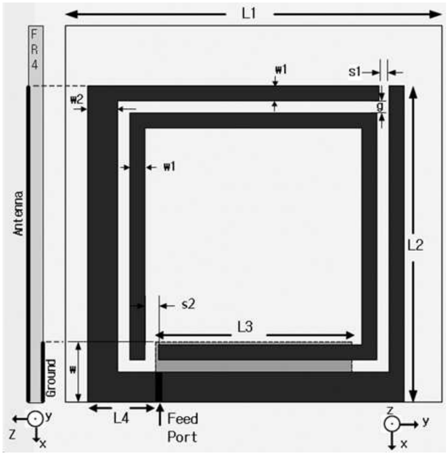

Figure 2. Proposed near-field antenna structure.

Table 1. Parameters of proposed antenna.

Antenna Square Edge (mm)	$L1$	25.0
SRR structure (mm)	$L2$	21.0
	$L4$	4.5
	$s1$	1.0
	$s2$	1.0
	$w1$	1.0
	$w2$	2.0
	g	0.8
Metal ground (mm)	$L3$	13.0
	W	4.0

On the bottom view, $L3$ is the long edge of the rectangle ground, and W is the short edge.

The dimensions of design parameters are presented in Table 1.

An antenna prototype was fabricated according to the dimensions of Table 1, as shown in Fig. 3. The entire area of antenna prototype is just one square inch ($25 * 25\,\text{mm}^2$), as a coin of 1 CNKY.

4. SIMULATION AND MEASUREMENT RESULTS

The comparison of simulated and measured S-parameter is shown in Fig. 4. Simulations of the proposed antenna were performed using Ansoft High Frequency Structure Simulator (HFSS) software, which uses the finite element method (FEM). The measured impedance bandwidth of the antenna prototype is 13 MHz (914.5–927.5 MHz) under the condition of reflection coefficient less than −10 dB, which agrees well with the simulated results and covers the China RFID Band II standard (920–925 MHz) completely.

Since the size of SMA connector is comparable to the proposed antenna in Fig. 3 and extends the ground in measurement, the measured result of S_{11} is better than the simulated result in Fig. 4. The antenna ground is often connected to the PCB in application, so we consider the effect of SMA connector equivalent to the effect of PCB ground. The measurement is more close to practical use rather than simulation.

The simulation result of current distribution is shown in Fig. 5. We can see the current remains constant along the outer square, which can provide a uniform magnetic field distribution and be suitable for near-field antenna.

As shown in Fig. 6, the magnetic near-field distribution of the antenna is simulated in both horizontal and vertical planes. Fig. 5(a)

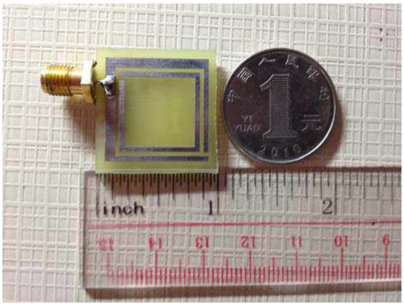

Figure 3. Photograph of the proposed antenna prototype.

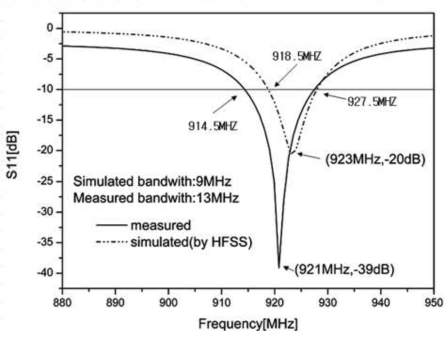

Figure 4. Photograph of the proposed antenna prototype.

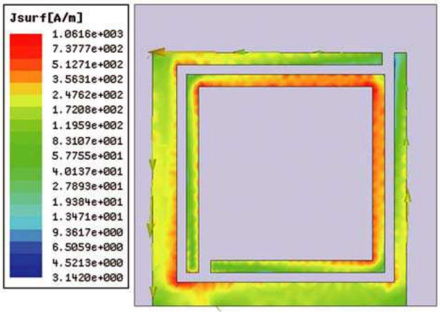

Figure 5. Simulated current distribution of the proposed antenna.

shows the magnetic field achieves 60 mm at the *yoz* plane, and Figs. 6(b)–(f) show the magnetic field above the antenna at different *xoy* planes. The interrogation zone in Figs. 6(b)–(f) is uniform on the most region of antenna, and agrees well with the simulation of current in phase along the antenna in Fig. 5.

Based on the fabricated prototype, we measure the read range of proposed antenna by using typical near-field RFID tag. The test scene is presented in Fig. 7(a). The reference tag is parallel to the surface of fabricated antenna, and the reading range d is achieved along the positive Z-axis. The Impinj UHF button [8] of $14 * 10\,\text{mm}^2$ dimension is shown in Fig. 7(b), which is taken as the reference near-field RFID tag for measurement.

In Fig. 8, the measured read width show that the reading distance of antenna prototype can reach 42 mm along the positive Z-axis, and the read width at XOY plane is 40 mm, 35 mm, 25 mm and 5 mm at $z = 20$ mm, $z = 30$ mm, $z = 40$ mm, and $z = 42$ mm, respectively. From Fig. 8, we can see that the reading width at $z = 20$ mm is similar with $z = 30$ mm, which agrees well with the simulated magnetic field

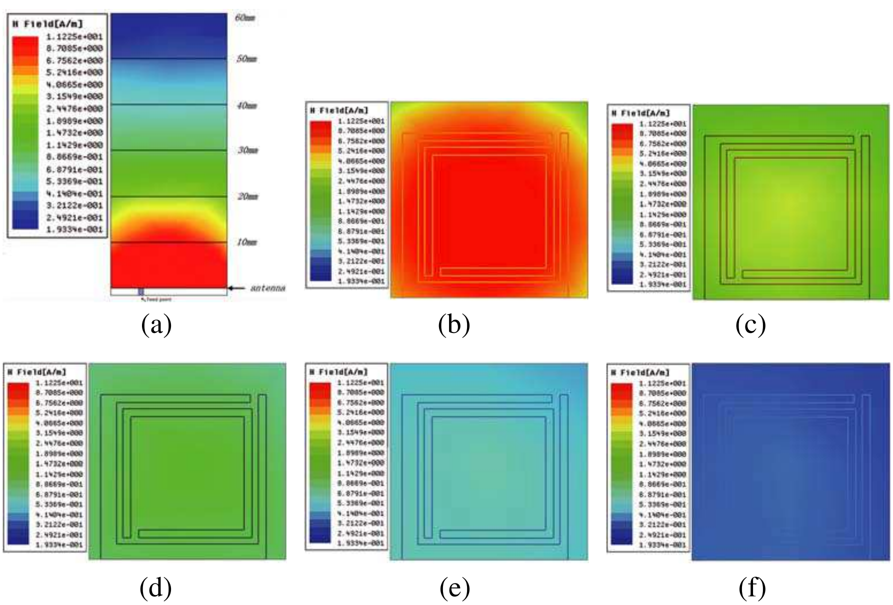

Figure 6. Simulated magnetic field distribution of the proposed antenna (a) at *yoz* plane, and in the near zone of (b) $z = 10$ mm, (c) $z = 20$ mm, (d) $z = 30$ mm, (e) $z = 40$ mm, (f) $z = 50$ mm, at *xoy* plane.

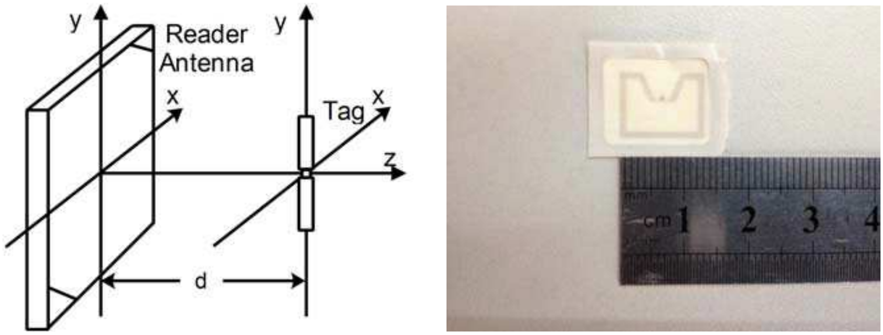

(a) (b)

Figure 7. Measurement environment. (a) Test scene of the proposed antenna. (b) Impinj UHF button.

Table 2. Comparison of maximum reading distance in different environment.

Environment	Reading range (mm)	
	Tx Power @10 dBm	Tx Power @20 dBm
Air	30	42
Water	42	56
Paper	33	36
Plant surface (corn)	37	38
Skin surface (human)	24	29

distribution. Since the simulated amplitude of magnetic field is below 0.4 A/m, the tag still can be read even on the 5 mm-wide zones at the $z = 42$ mm plane.

Furthermore, the reading distance is measured under the different environment. From Table 2, we can see the measured results with the same tag attached on the surface of different objects, including air, liquids, paper, Plant and human body surface. When the tag is attached to a book (paper), or an apple (plant), the reading range is still similar with air. Even the reading result is better with the tag attached to a water-item container (liquid). Additionally, the reading range is only reduced by 20% when tag is attached to a large conducting plate, such as skin of human being. Therefore, different environment did not seriously affect the reading performance, which is a major

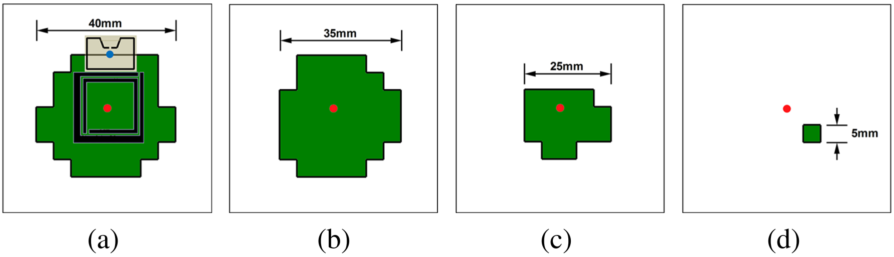

Figure 8. Measured read width at *xoy* plane: (a) $z = 20$ mm. (b) $z = 30$ mm. (c) $z = 40$ mm. (d) $z = 42$ mm.

Table 3. RFID spectrums worldwide.

Region		Frequency Spectrum
North America (USA. & Canada)		902–928 MHz
Europe		865–868 MHz
China	Band I	840–845 MHz
	Band II	920–925 MHz
Korea		917–924 MHz
Australia		918–926 MHz

advantage of near-field RFID antenna.

In addition to miniaturization, another interesting advantage of the proposed antenna is the customizability for RFID frequency spectrum of different regions. Most of the regions all over the world have different frequency spectrums for RFID application, just as communication application. The RFID device, including RFID reader antenna, must be suitable for the local frequency spectrums. The RFID spectrums of the main regions in the world are listed in Table 3 [15].

As shown in Fig. 8, the proposed antenna can be customized for three kinds of RFID bands by varying the structure parameter.

It is seen in Fig. 9, the proposed antenna can be customized for three kinds of RFID bands by varying the structure parameter. The antenna has an enough bandwidth for China RFID Band I (840–845 MHz), with $g = 0.6$ mm, $s1 = 1.1$ mm, and $s2 = 0.4$ mm. On the other hand, if the parameter $s2$ is enhanced with a larger value of 0.9 mm, the bandwidth of antenna will be customized for Europe RFID Band (865–868 MHz). Finally, the antenna, which covers China RFID Band II (920–925 MHz), is the same antenna in Fig. 2, and Table 1. This antenna bandwidth (914.5–927.5 MHz) is also suitable

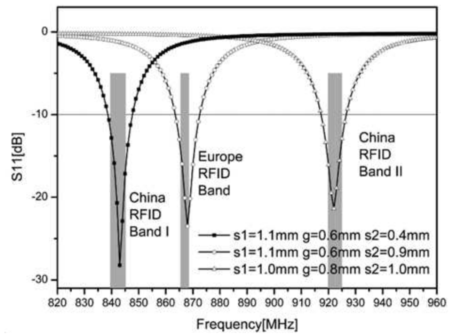

Figure 9. Effect of the varying antenna structure parameters for RFID frequency spectrum.

for Korea RFID Band (917–924 MHz) and Australia RFID Band (918–926 MHz). But the bandwidth is too narrow to cover completely the North America Band (902–928 MHz). Therefore, the expended bandwidth of the proposed antenna will be the next focus for the future research.

5. CONCLUSIONS

In this paper, the proposed antenna uses two SRRs to obtain a small dimension of $21 * 21 * 1.6\,\text{mm}^3$. From Table 1 and Fig. 4, the edge of the antenna outer ring is 21 mm, which is approximately equal to 1/16 wavelength at 920 MHz, and the edge of the classical patch antenna must be 163 mm, which is about 1/2 wavelength at 920 MHz. Thus, the proposed antenna is one of the smallest RFID reader antennas all over the world, which is suitable for mobile application. Moreover, the parameters of SRR structure can be modified to handle different UHF RFID bands (Europe band, China band I&II).

Finally, a proposed antenna prototype is fabricated and detects passive UHF RFID tag in near region successfully. It provides the reading range of 42 mm and bandwidth of 13 MHz (914.5–927.5 MHz) with reflection coefficient less than -10 dB, which can cover the China RFID band II (920–925 MHz) completely.

ACKNOWLEDGMENT

This paper is supported by the National High Technology Research and Development Program (863 program) of China (2008AA04A103), and the National Natural Science Foundation of China (61101015).

REFERENCES

1. Finkenzeller, K., *RFID Handbook: Radio-Frequency Identification Fundamentals and Applications*, 2nd Edition, Wiley & Sons, New York, 2004.
2. Nikitin, P. V., K. V. S. Rao, and S. Lazar, "An overview of near field UHF RFID," *Proc. IEEE Int. Conf. on RFID*, 167–174, Mar. 2007.
3. Qing, X., C. K. Goh, and Z.-N. Chen, "Segmented loop antenna for UHF near-field RFID applications," *Electron. Lett.*, Vol. 45, No. 17, 872–873, Aug. 2009.
4. Qing, X., C. K. Goh, and Z. N. Chen, "A broadband UHF near-fi eld RFID antenna," *IEEE Trans. Antennas Propag.*, Vol. 58, No. 12, 3829–3838, Dec. 2010.
5. Liu, H.-W., K.-H. Wu, and C.-F. Yang, "UHF reader loop antenna for near-field RFID applications," *Electron. Lett.*, Vol. 46, No. 1, 10–11, Jan. 2010.
6. Li, X., J. Liao, Y. Yuan, and D. Yu, "Eye-shaped segmented reader antenna for near-field UHF RFID applications," *Progress In Electromagnetics Research*, Vol. 114, 481–493, 2011.
7. Shrestha, B., A. Elsherbeni, and L. Ukkonen, "UHF RFID reader antenna for near-field and far-field operations," *IEEE Antennas Wireless Propag. Lett.*, Vol. 10, 1274–1277, Nov. 2011.
8. Li, X. and Z. Yang, "Dual-printed-dipoles reader antenna for UHF near-field RFID applications," *IEEE Antennas Wireless Propag. Lett.*, Vol. 10, 239–242, 2011.
9. Dobkin, D. M., S. A. Weigand, and N. Iyer, "Segmented magnetic antennas for near-field UHF RFID," *Microw. J.*, Vol. 50, No. 6, 96–102, Jun. 2007.
10. Kim, Y.-J., J.-H. Kim, and H.-M. Lee, "Electrically small square loop antenna with a capacitive SRR cover structure," *38th European Microwave Conference*, 893–896, Oct. 2008.
11. Kang, J.-J. and D.-J. Lee, "Compact mobile RFID antenna design and analysis using photonic-assisted vector near-field characterization," *IEEE International Conference on RFID*, 81-88, 2008.
12. Chao, J. W., Z. M. Xie, and X. Z. Lai, "A compact near field UHF RFID reader antenna using SRR," *International Conference on Machine Learning and Cybernetics*, Vol. 1, 330–332, Jul. 2011.
13. Pendry, J. B., A. J. Holden, D. J. Robbins, and W. J. Stewart, "Magnetism from conductors and enhanced nonlinear phenom-

ena," *IEEE Trans. Microw. Theory Tech.*, Vol. 47, No. 11, 2075–2084, Nov. 1999.

14. Si, L.-M. and X. Lv, "CPW-fed multi-band omni-directional planar microstrip antenna using composite metamaterial resonators for wireless communications," *Progress In Electromagnetics Research*, Vol. 83, 133-146, 2008.
15. "UHF for RFID Regulations," available at http://www.gs1.org/docs/epcglobal/UHF_Regulations.pdf.